



# Thermodynamics and Kinetic Investigation of Reaction of Acriflavine with L-cysteine in Aqueous Medium

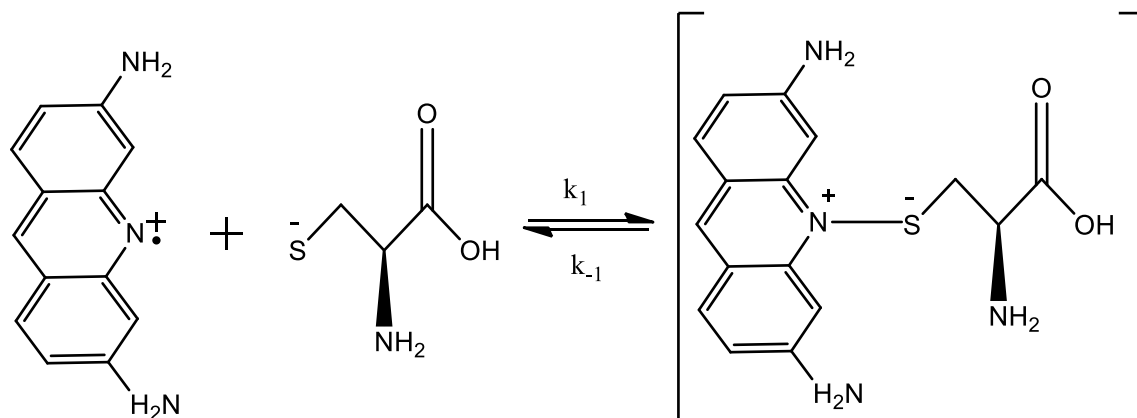
I. U. Nkole<sup>1</sup> · S. O. Idris<sup>1</sup>

Received: 30 March 2021 / Accepted: 10 September 2021 / Published online: 29 September 2021  
© The Tunisian Chemical Society and Springer Nature Switzerland AG 2021

## Abstract

The kinetic investigation of reaction of 3,6-diamino-10-methylacridin-10-ium chloride (acriflavine) with L-cysteine in aqueous acidic medium at maximum absorption = 460 nm, ionic strength (I) = 0.1 mol dm<sup>-3</sup> and temperature (T) = 307 K has been carried out spectrophotometrically. Using a pseudo first order approach, the rate of the redox reaction resulted to first order with respect to the [acriflavine, (AF)] and [L-cysteine, (CSH)] and second order total. Stoichiometric determination confirms that a mole of the acriflavine is consumed by a mole of L-cysteine at a time for the attainment of product formation. The reaction followed a one-way acid independence path. The adjustment in ionic strength (NaCl) and solvent polarity (water/acetone mixture) of the reaction system showed no reasonable effect and there was a fairly decrease in the reaction rate, respectively. The reaction rate is also characterised by neither catalysis nor inhibition of added ions. The negative magnitude of entropy of activation,  $\Delta S^\ddagger$ , ( $-151.39 \pm 031 \text{ J mol}^{-1} \text{ K}^{-1}$ ) and positive value of enthalpy of activation,  $\Delta H^\ddagger$ , ( $+31.378 \pm 030 \text{ kJ mol}^{-1}$ ) suggest that the reaction proceeds via an associative pathway and reasonable energy are needed to lower the activation energy for a tangible products formation. Two acridine unit products polymerised afterward forming a dimer as a result of an intramolecular coupling. A determinable intermediate has been observed through a spectroscopic test and confirmed by Michaelis–Menten's plot. Based on Taube's inorganic electron transfer reaction, an inner-sphere mechanistic pathway is implicated with a stable intermediate complex formation as shown below;

## Graphic abstract



**Keywords** Kinetics · Acriflavine · Thermodynamic · L-cysteine · Mechanism

✉ I. U. Nkole  
iunkole@abu.edu.ng; nkoleikechukwu@gmail.com

<sup>1</sup> Department of Chemistry, Ahmadu Bello University, Zaria, Nigeria

## 1 Introduction

Acriflavine (3,6-diamino-10-methylacridin-10-ium chloride) is a topical antiseptic dye derived from acridine with a  $\pi$ -conjugated structure in its backbone. It was used to counter sleeping sickness. It is used in fluorescently labelling of high molecular weight ribonucleic acid (RNA), genetically active agent, antibacterial agent, and anticancer agent [1, 2]. It has been reported to inhibit the development of asexual phases of both chloroquine-sensitive and resistant strains of the human malarial parasite, *plasmodium falciparum in-vitro* at nano-molar concentration [3]. Likewise, it has also been documented that acriflavine overturns the propagation of tumour cells. The anti-tumour and anticancer effects of acriflavine have been reported in a variety of biological systems [4, 5]. The identification of acriflavine as an active papain-like protease inhibitor for countering COVID-19 caused by SARS-CoV-2 is promising and essential in the sense that it inhibits viral replication in cellular models of mice (in vivo) and human (ex vivo) airway epithelia cultures. Its actions on the active site of the enzyme involve an unprecedented binding mode by blocking the virus infection outside a living organism (in vitro) [6–10].

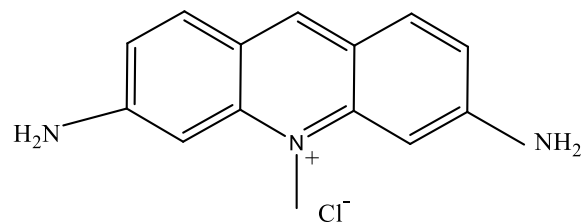
Compounds with thiol group are readily oxidised to disulphide and sulfenic acid, and this resulted in their frequent biological investigations [11]. Thus, l-cysteine (CSH) is a semi-essential proteinogenic amino acid that plays a vital role in protein denaturation and an essential part of enzymes. Its thiol group (–SH), thiolate ion (CS<sup>–</sup>), and thiyl radical species (CS<sup>\*</sup>) are capable of initiating reduction reaction in acidic, aqueous, or buffer media [11–13]. The electron transfer reactions of l-cysteine have been investigated in a good number of researches such as reduction of trinuclear Mn(IV) species in which the rate was found to increase in aqua media [14], [Mn<sub>4</sub>O<sub>6</sub>]<sup>4+</sup> core resulted in a significant decrease in the observed second-order rate constants in aqua media enriched with deuterium water and a proton-mixed single electron transfer reaction was proposed [15], 11-tungstophosphovanate(V) resulted in a first order with respect to [redox species] [16], Hexacyanoferrate(III) showed an increased reaction rate with increase in hydroxide ion concentration and the product was found to be sulfenic acid [17], and [CoSalophen]<sup>+</sup> complex established the importance of deprotonated and protonated form of l-cysteine in the electron transfer process [18]; in the view to gain more understanding of the character of enzymes containing thiol group in bio-systems.

However, the knowledge of probable side-reaction of acriflavine in cellular models prompted this study in order to understand the working mechanism of it on SARS-CoV-2, cancer progression and tumour-stromal interplay in temperature-regulated media. Also, this study is to understand the chemistry of the sulfhydryl group of the l-cysteine (–SH) with that of the acridine and diamine side chain of acriflavine in an aqueous medium in order to expand the frontier of knowledge on the biological importance of thiols like cysteine in living cells.

## 2 Experimental

### 2.1 Materials

Acriflavine, Scheme 1, and l-cysteine were obtained from Sigma-Aldrich, Germany. Sodium chloride, NaCl, (BDH, United Kingdom, UK) was used to keep the reaction's ionic strength constant. Calcium chloride, CaCl<sub>2</sub>, (BDH, UK) and sodium sulphate, Na<sub>2</sub>SO<sub>4</sub>, (May and Baker, Nigeria) were used to ascertain the effect of additives (added ion) on the reaction rate. Hydrochloric acid, HCl, (BDH, UK) was used to study the effect of [H<sup>+</sup>] on the rate of reaction. Acetone (May and Baker, Nigeria) was used to investigate the effect of solvent polarity (dielectric constant) on the reaction mixture. Hydrogen peroxide (BDH, UK) was used as part of the product analysis. Acrylamide with methanol (May and Baker, Nigeria) was used to check the participation of unstable atoms in the reaction. Kinetic investigations were performed with a SHERWOOD Colorimeter Model 254 and a Grant JB1 thermostated water bath was used to maintain the temperature. UV/Visible spectrophotometer (Double Beam Cary 300 Series UV–Vis Spectrophotometer, Agilent Technologies, USA) and FTIR (FTIR-8400S Fourier Transform Infrared Spectrophotometer, Shimadzu, Double Beam) were used for characterisation of acriflavine and reaction products.



**Scheme 1** The structure of acriflavine (AF)

## 2.2 Stoichiometry

The stoichiometry of the reaction was determined spectrophotometrically under the reaction condition  $[AF] = 3.6 \times 10^{-5}$  M,  $[CSH] = (0.72 - 14.4) \times 10^{-5}$  M,  $I = 0.1$  mol  $\text{dm}^{-3}$  and  $T = 307$  K. For a series of solutions containing constant  $[AF]$ , the  $[CSH]$  was varied and the absorbance of the reaction mixtures were measured for an interval of six (6) hours after the initial measurement before arriving at constant absorbance at the fourth interval [19, 20].

## 2.3 Kinetic Measurement

The reaction order was determined by observing the bleaching of the reaction system as the reaction proceed at a maximum absorbance = 460 nm. The process was done using pseudo-first-order settings with the  $[CSH]$  100-fold in excess over  $[AF]$  at a constant ionic strength of 0.1 mol  $\text{dm}^{-3}$  (NaCl). Graphs of absorbance ( $A$ ) against time ( $t$ ) was done for all the folds (550 – 1000), and the observed rate constants,  $k_1$  were obtained as the gradients of the graphs represented by Eq. 1:

$$\frac{A_t}{A_0} = \exp(-kt) \quad (1)$$

where  $A_t$  and  $A_0$  are the absorbances at the time  $t$ , and 0 respectively,  $k$  is the observed rate constant and  $t$  is the time (seconds). The second-order rate constants,  $k_2$  were determined from Eq. 2:

$$k_2 = k_1/[CSH] \quad (2)$$

The effect of hydrogen ion concentration was determined by a change 0.001–0.008 M, the salt effect of reaction medium within the range of 0.1 – 0.8 mol  $\text{dm}^{-3}$  (NaCl), and the solvent polarity was varied by the addition of acetone (0.04 – 0.32  $\text{cm}^3$ ) at constant concentrations of the reactants and temperature of 307 K [19, 21, 22].

## 2.4 Effect of Added Ions on the Rate of Reaction

The effect of added ions was investigated under a constant concentration of oxidant, reductant, ionic strength, and at  $[X^{2\pm}] = 3.0 - 27 \times 10^{-4}$  M [23–25].

## 2.5 Test for Free Radical Species and Product Intermediate Complex

The investigation of the existence of unstable atoms in the reaction mixture was carried out by adding 0.4  $\text{cm}^3$  of acrylamide solution (0.1 M) to an incompletely reacted acriflavine mixture and excess methanol [26–29].

The product intermediate complex was examined spectroscopically by scanning the partially reacted mixture at wavelength 400–800 nm, and Michaelis–Menten's plot of  $k_1^{-1}$  against  $[CSH]^{-1}$  was equally done [30, 31].

## 2.6 Temperature Dependence Investigation

The impact of temperature on the system mixture was done by changing the temperature at six different degrees (307 – 327) K, and all other conditions were fixed. The activation parameters for the second-order rate constant ( $k_2$ ) were evaluated by means of Eyring–Polanyi Eq. 3.

$$\ln\left(\frac{k_2}{T}\right) = \ln\left(\frac{K_b}{h}\right) + \frac{\Delta S^\ddagger}{R} - \frac{\Delta H^\ddagger}{RT} \quad (3)$$

where  $K_b$  is Boltzmann's constant,  $h$  is Planck's constant,  $k_2$  is second rate constant,  $T$  is temperature,  $R$  is gas constant,  $\Delta S^\ddagger$  is the entropy of activation and  $\Delta H^\ddagger$  is the enthalpy of activation. The  $\Delta S^\ddagger$  and  $\Delta H^\ddagger$  were calculated from the intercept and gradient of the plot of  $\ln\left(\frac{k_2}{T}\right)$  against  $\frac{1}{T}$  [23].

## 2.7 Analysis of the Product

Excess methanol was introduced at the end of the reaction, and a separation funnel was used to separate the two layers (gelatinous and non-gelatinous layers) that were formed. Fourier Transform Infrared (FTIR) spectroscopic was run for the gelatinous layer, and the UV–Visible spectrum of the l-cysteine (CSH) treated with two drops of 5% hydrogen peroxide was compared with the spectrum of the non-gelatinous layer of the reaction product [2, 18].

## 3 Results and Discussion

### 3.1 Stoichiometry and Product Analysis

The stoichiometric titration shows that two moles of acriflavine required two moles of l-cysteine in the course of the reaction, and it is represented by Eq. 3 and Fig. 1;

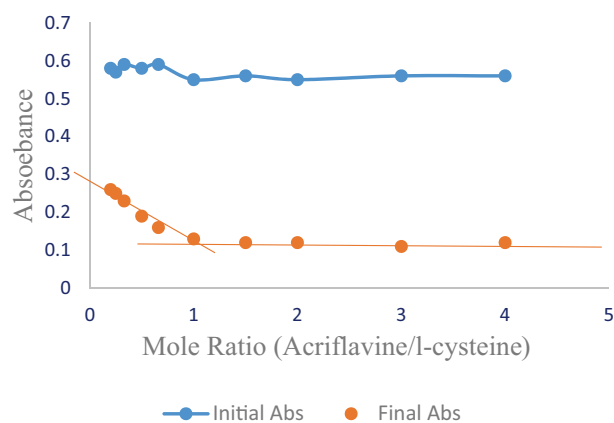


**Fig. 1** Stoichiometric plot of the reaction of acriflavine with l-cysteine at  $[AF]=3.6\times 10^{-5}$  M,  $I=0.1$  mol  $\text{dm}^{-3}$  (NaCl),  $[CSH]=(0.72 - 14.4)\times 10^{-5}$  M,  $\lambda_{\text{max}}=460$  nm, and  $T=307$  K

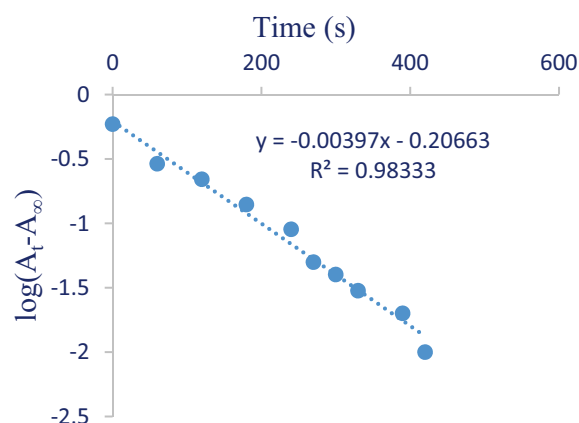
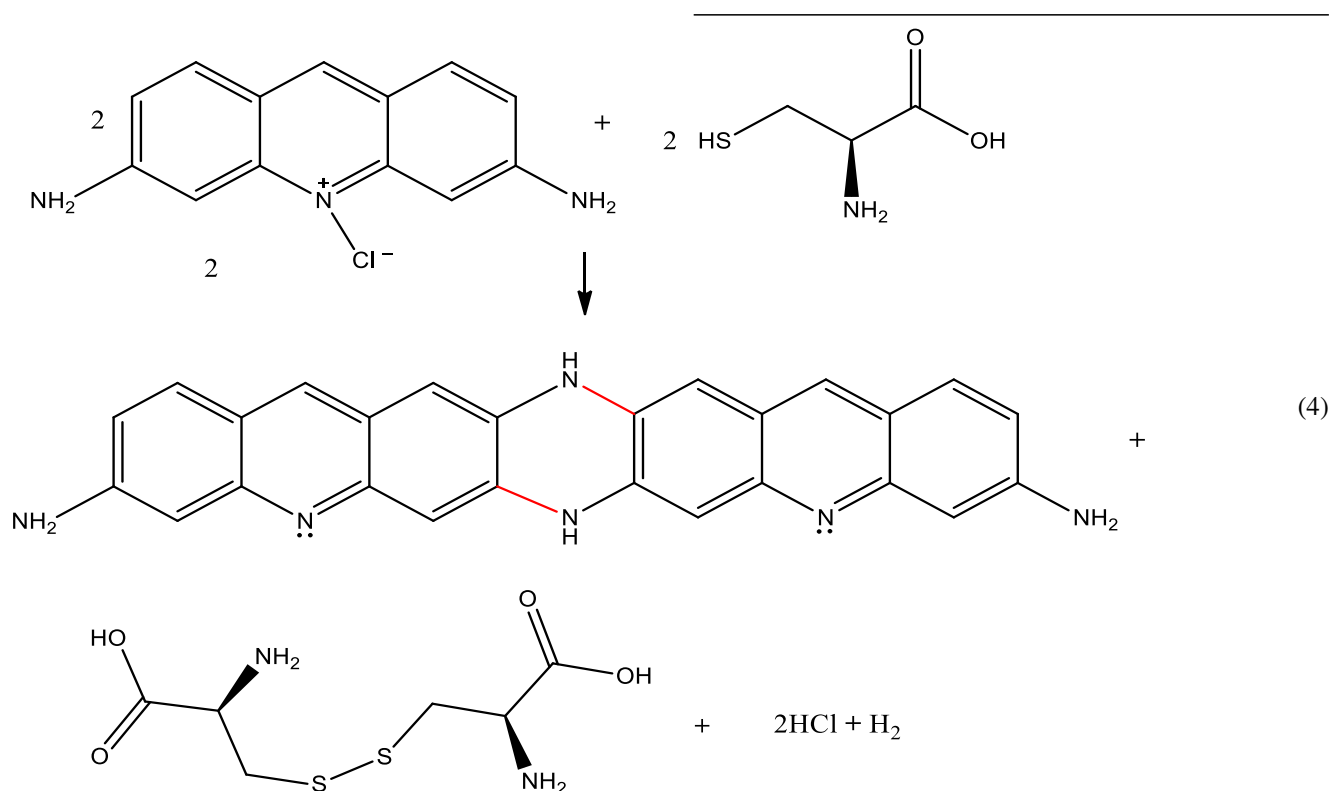


**Fig. 2** Pseudo-first-order plot for the reaction of acriflavine and l-cysteine at  $I=0.1$  mol  $\text{dm}^{-3}$ ,  $\lambda_{\text{max}}=460$  nm, and  $T=307$  K



The result of the stoichiometry is in the similitude of the previous report in the reduction of  $N,N'$ -phenylenebis(salicylideneiminato)cobalt(III) by l-cysteine [18].

The FTIR spectroscopy of acriflavine shows  $3022\text{ cm}^{-1}$   $\nu(\text{C-H})$  phenyl,  $1628\text{ cm}^{-1}$   $\nu(\text{C=N})$  aromatic ring,  $1598\text{ cm}^{-1}$   $\nu(\text{C=C})$  phenyl,  $1321\text{ cm}^{-1}$   $\nu(\text{C-N})$ ,  $3310\text{--}3164\text{ cm}^{-1}$   $\nu(\text{N-H})$ , and that of polymerised acridine

includes  $3030\text{ cm}^{-1}$   $\nu(\text{C-H})$  phenyl,  $1658\text{ cm}^{-1}$   $\nu(\text{C=N})$  aromatic ring,  $1597\text{ cm}^{-1}$   $\nu(\text{C=C})$  phenyl,  $3152\text{ cm}^{-1}$   $\nu(\text{N-H})$ .

The stretching band of the aromatic C-H bond at  $3022\text{ cm}^{-1}$  was detected at  $3030\text{ cm}^{-1}$  in the dimer assembly of acridine. The sharp absorption peaks at  $1622$  and  $1594\text{ cm}^{-1}$  corresponded to the C=N and C=C stretching bands for acriflavine, which became broader ( $1658$  and  $1597\text{ cm}^{-1}$ , respectively) due to an enhancement in conjugation after polymerisation. The absorption peaks at  $3310$  and

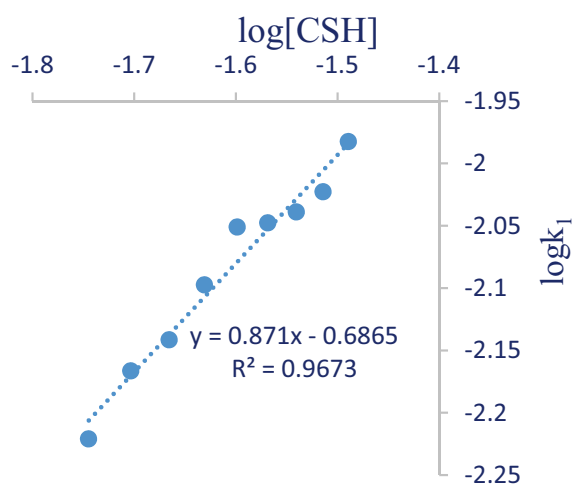


**Fig. 3** Plot of  $\log k_1$  against  $\log[\text{CSH}]$  for the reaction of acriflavine and l-cysteine at  $I=0.1 \text{ mol dm}^{-3}$ ,  $\lambda_{\text{max}}=460 \text{ nm}$ , and  $T=307 \text{ K}$

**Table 1** Second-order and pseudo-first-order rate constants for the reaction of acriflavine with l-cysteine at  $[\text{AF}]=3.6 \times 10^{-5} \text{ M}$ ,  $T=307 \text{ K}$  and  $\lambda_{\text{max}}=460 \text{ nm}$

$10^2[\text{CSH}], \text{M}$	$I, \text{mol dm}^{-3}$	$10^3 k_1, \text{s}^{-1}$	$10^1 k_2, \text{M}^{-1} \text{s}^{-1}$
1.80	0.10	6.01	3.33
1.98	0.10	6.81	3.44
2.16	0.10	7.21	3.34
2.34	0.10	7.99	3.41
2.52	0.10	8.89	3.52
2.70	0.10	8.95	3.31
2.88	0.10	9.14	3.17
3.06	0.10	9.48	3.10
3.24	0.10	10.4	3.21
2.88	0.10	9.14	3.17
2.88	0.20	8.91	3.09
2.88	0.30	9.02	3.13
2.88	0.40	9.09	3.15
2.88	0.50	8.63	2.99
2.88	0.60	9.09	3.15
2.88	0.70	9.12	3.16
2.88	0.80	9.14	3.17
2.88	0.90	8.93	3.10

**Table 2** Effect of solvent polarity on the rate of reaction of acriflavine and l-cysteine at  $[\text{AF}]=3.6 \times 10^{-5} \text{ M}$ ,  $[\text{SCH}]=2.88 \times 10^{-2} \text{ M}$ ,  $I=0.1 \text{ mol dm}^{-3}$ ,  $T=307 \text{ K}$  and  $\lambda_{\text{max}}=460 \text{ nm}$

D	80.1	79.3	78.6	77.9	77.2	76.5	75.7	75.0	74.3
$10^3 k_1 (\text{s}^{-1})$	9.14	8.77	8.65	8.45	8.22	8.03	7.87	7.76	7.66
$10^1 k_2 (\text{M}^{-1} \text{s}^{-1})$	3.17	3.04	3.00	2.95	2.85	2.79	2.73	2.69	2.66

$3164 \text{ cm}^{-1}$  which is ascribable to the N–H stretching modes of the  $-\text{NH}_2$  groups are substituted by one broader peak at  $3152 \text{ cm}^{-1}$  for the dimer acridine units which indicates the conversion of the  $1^0$  amine to a  $2^0$  amine through polymerisation that took place on N-atoms of  $1^0$  amine groups that changed to the C–N coupled unit.

The correspondence of UV–Visible spectra of the l-cysteine (CSH) treated with two drops of 5%  $\text{H}_2\text{O}_2$  and that of the non-gelatinous layer of the reaction product is indicative of successful oxidation of the thiol in the reaction mixture to disulphide.

### 3.2 Reactions Order and Rate Constant

The reaction resulted in a first order with respect to the  $[\text{AF}]$  due to consecutive linearity of the graphs of  $\log(A_t - A_\infty)$  against time and a typical one is shown in Fig. 2, and first-order with respect to the concentration of CSH as proven by the logarithmic plot of  $k_1$  against  $[\text{CSH}]$  that is one-dimensional with a slope of 0.871 and a correlation coefficient  $R^2=0.9673$  (Fig. 3) which is reinforced by the consistency of the  $k_2$  in Table 1.

### 3.3 Salt and Solvent Polarity Effects

The salt effect on the reaction mixture was not noticeable on the rate of the reaction which is an indication of neutral Brønsted salt effect interplay (Table 1 and Fig. 4), and this is reinforced by a fair decrease in the reaction rate as the solvent polarity of the reaction mixture decreases (Table 2). This suggests that the strength of the intermolecular hydrogen bonds between the  $-\text{NH}$  group of acriflavine and the  $-\text{OH}$  functional group of the solvent moiety influenced it.

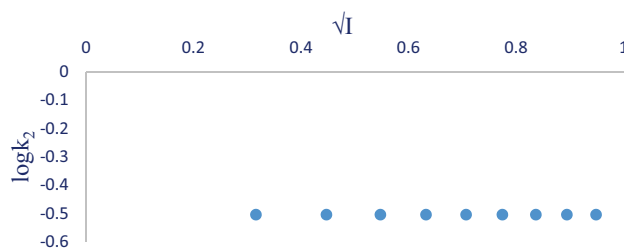


**Fig. 4** Plot of  $\log k_2$  versus  $\sqrt{I}$  for the reaction of acriflavine and l-cysteine at  $\lambda_{\text{max}}=460 \text{ nm}$ , and  $T=307 \text{ K}$ ,  $I=(0.1 - 0.9) \text{ mol dm}^{-3}$

**Table 3** Effect of additives on the rate of reaction of acriflavine and l-cysteine at  $[AF] = 3.6 \times 10^{-5}$  M,  $[SCH] = 2.88 \times 10^{-2}$  M,  $I = 0.1$  mol dm $^{-3}$ ,  $T = 307$  K and  $\lambda_{\max} = 460$  nm

$10^4[Ca^{2+}]$ M	$10^3k_1$ s $^{-1}$	$10^1k_2$ M $^{-1}$ s $^{-1}$	$10^4[SO_4^{2-}]$ M	$10^3k_1$ s $^{-1}$	$10^1k_2$ M $^{-1}$ s $^{-1}$
3.0	9.14	3.17	3.0	9.14	3.17
6.0	9.12	3.16	6.0	9.09	3.15
9.0	9.14	3.17	9.0	9.16	3.18
12.0	9.09	3.15	12.0	9.09	3.15
15.0	9.14	3.17	15.0	9.18	3.19
18.0	9.09	3.15	18.0	9.12	3.16
21.0	9.12	3.16	21.0	9.14	3.17
24.0	9.16	3.18	24.0	9.09	3.15
27.0	9.12	3.16	27.0	9.14	3.17

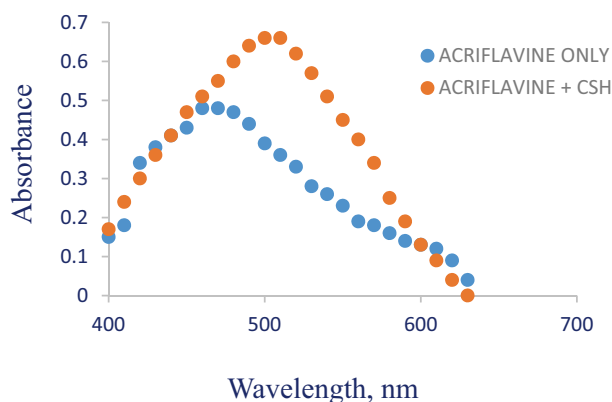


**Fig. 5** Spectrum of acriflavine and the reaction mixture of acriflavine and l-cysteine

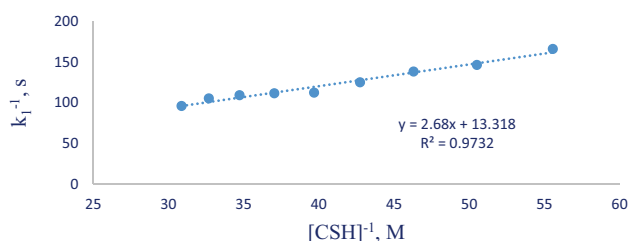


**Fig. 6** Michaelis–Menten's plot of  $k_1^{-1}$  against  $[CSH]^{-1}$

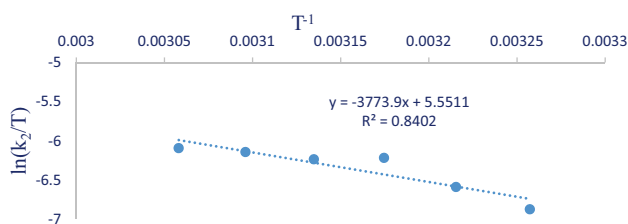


**Fig. 7** Graph of  $\ln(k_2/T)$  against  $T^{-1}$

### 3.4 Other Determinations

The influence of hydrogen ion concentration on the rate of reaction was negative which is an indication of a reaction taking place through an independent hydrogen ion concentration [29].

The introduction of additives ( $Ca^{2+}$  and  $SO_4^{2-}$  ions) into the reaction mixture has an insignificant influence on the rate of reaction (Table 3), and this suggests the possibility of a neutral intermediate complex at the slow step (Eq. 7).

The participation of unstable atoms in the reaction was positive as there was a polymerisation of the acrylamide in the incompletely reacted acriflavine/l-cysteine mixture when excess methanol was added.

The spectroscopic investigation of the intermediate complex showed a reasonable shift in  $\lambda_{\max}$  as shown in the spectrum of the partially reacted mixture (Fig. 5) which is an indication of the presence of stable intermediate complex formation, and this is supported by the linearity of Michaelis–Menten's plot of  $k_1^{-1}$  against  $[CSH]^{-1}$  with an intercept (Fig. 6) which is one of the kinetic evidence used in ascertaining the possibility of existence of detectable intermediate complex. This further confirms a reaction proceeding through an inner-sphere mechanistic pathway.

### 3.5 Determination of Activation Parameters

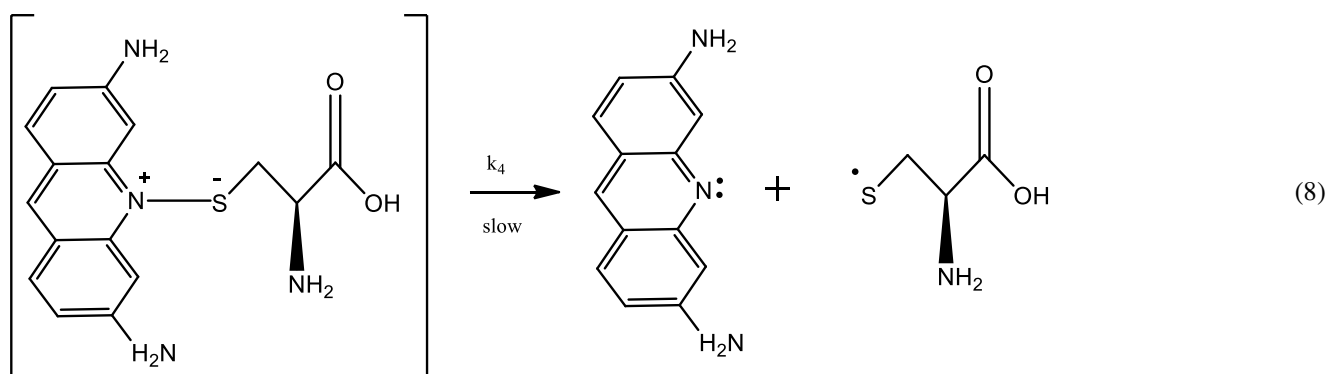
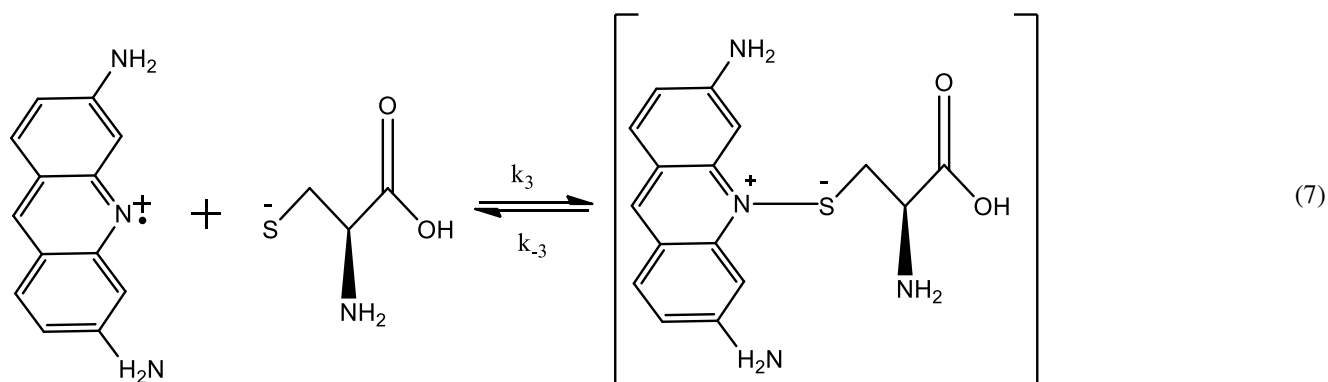
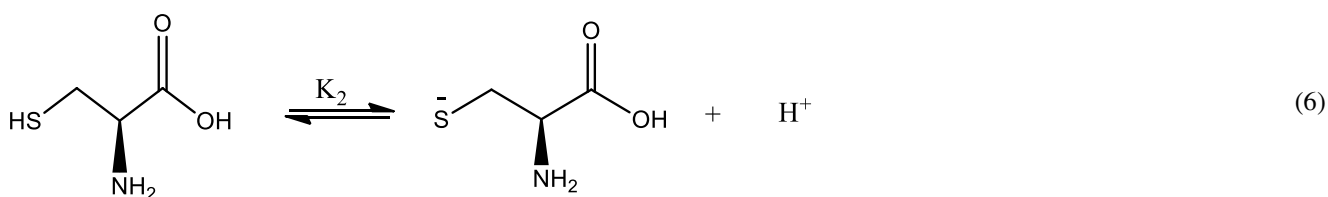
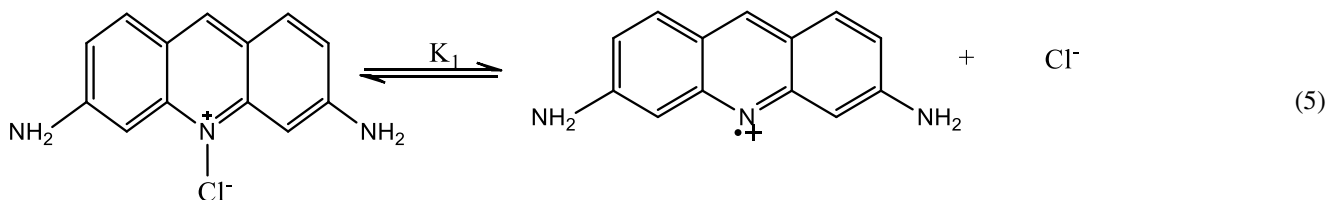
The effect of change in temperature of the reaction mixture (Fig. 7) resulted in a negative magnitude of  $\Delta S^\ddagger$  ( $-151.39 \pm 031$  J mol $^{-1}$  K $^{-1}$ ) and a positive value of  $\Delta H^\ddagger$  ( $+31.378 \pm 030$  kJ mol $^{-1}$ ) which suggest that the activated complex is more ordered than the reacting species and is indicative of an associative process which points to the inner-sphere mechanism. The value of activation energy,  $E_a$ , ( $28.82 \pm 030$  kJ mol $^{-1}$ ) shows that the product formation was fairly fast since  $E_a$  is relatively lower than  $\Delta H^\ddagger$ . The  $\Delta G^\ddagger$  ( $+77.85 \pm 030$  kJ mol $^{-1}$ ) reinforced the occurrence of an endothermic process during the reaction.

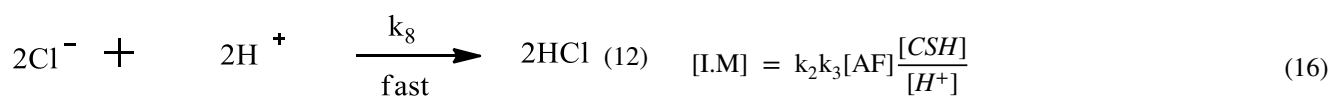
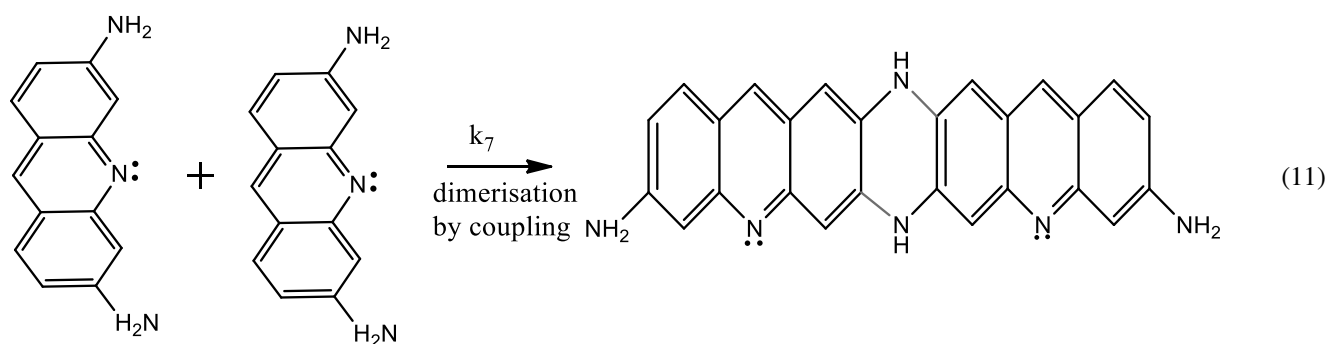
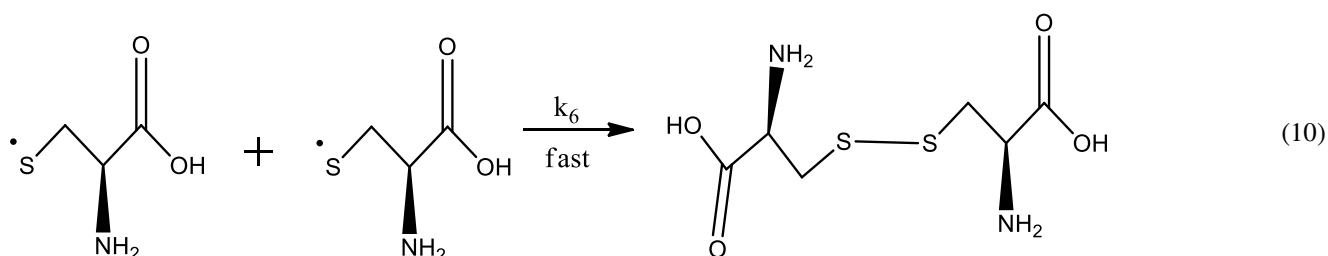
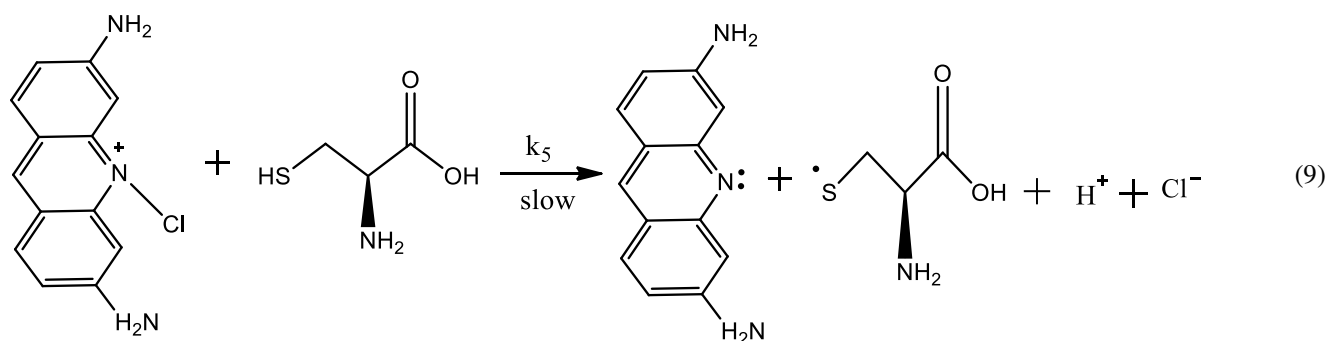
### 3.6 Reaction Mechanism

Owing to kinetic and non-kinetic parameters obtained in this investigation, an inner-sphere mechanism (Eqs. 5–12) is presented for this reaction on the evidence that:

(1) Michaelis–Menten's plot (Fig. 6) of  $k_1^{-1}$  against  $[\text{CSH}]^{-1}$  was linear with a reasonable intercept.

- (2) The spectrophotometric scanning of the reaction mixture showed a significant shift in  $\lambda_{\text{max}}$  (Fig. 5).  
 (3) Added cation and anion did not have an effect on the rate of reaction.  
 (4) The negative value of  $\Delta S^\ddagger$  has been ascribed to reactions occurring via an inner-sphere mechanism.





$$\text{Rate} = k_4 [\text{I.M}] + k_5 [\text{AF}] [\text{CSH}] \quad (13)$$

where

$$[\text{I.M}] = k_3 [\text{AF}] [\text{CS}^-] \quad (14)$$

from Eq. 6,

$$[\text{CS}^-] = K_1 \frac{[\text{CSH}]}{[\text{H}^+]} \quad (15)$$

Substituting Eq. 15 into 14;

Substituting Eq. 16 into 13;

$$\text{Rate} = k_3 k_4 K_1 [\text{H}^+]^{-1} [\text{AF}] [\text{CSH}] + k_5 [\text{AF}] [\text{CSH}] \quad (17)$$

$$\text{Rate} = k_3 k_4 K_1 [\text{H}^+]^{-1} + k_5 [\text{AF}] [\text{CSH}] \quad (18)$$

$$\text{Rate} = k [\text{AF}] [\text{CSH}] \quad (19)$$

where

$$k = k_3 k_4 K_1 [\text{H}^+]^{-1} + k_5 \quad (20)$$

also, [I.M] = Intermediate complex in Eq. 7.

## 4 Conclusion

Thermodynamics and kinetic investigation of the reaction of acriflavine with L-cysteine in an aqueous medium have been studied. It was found that the order of the reaction with respect to the concentration of acriflavine and L-cysteine is first order and second-order overall. It was established that one mole of acriflavine requires a mole of L-cysteine for the product formation, and the reaction proceeds through an associative pathway, and a lowered activation energy is necessary for an enhanced product formation. The dimerisation of acridine product revealed the significance of intramolecular coupling in physiochemical and biochemical processes, and the sulfhydryl group of the L-cysteine (–SH) was imperative in initiating and activating the reaction to the transition state and product. The participation of an intermediate complex as a mechanistic route director in biochemical activities is one of the driving forces in understanding complex reaction systems, and its role is key in a wide variety of metabolic and cellular processes. The study further buttresses the important of free atoms (radicals) in bio-system and nuclear reactor that can lead to formation of macromolecules.

**Funding** This study did not receive any definite contribution from funding agencies in the public, commercial or private sector.

## Declarations

**Conflict of interest** The authors declare that they have no conflict of interest.

## References

- Lee K, Zhang H, Qian DZ, Rey S, Liu JO, Semenza GL (2009) Acriflavine inhibits HIF-1 dimerisation, tumor growth, and vascularisation. *Proc Natl Acad Sci* 106(42):17910–17915
- Kolcu K, Kaya I (2017) Synthesis, characterisation and photovoltaic studies of oligo(acriflavine) via chemical oxidative polymerisation. *Roy Soc Chem Adv* 7:8973–8984. <https://doi.org/10.1039/c6ra28475brsc.li/rsc-advances>
- Lerman LS (1963) The structure of the DNA-acridine complex. *Proc Natl Acad Sci* 49:94–102
- Doudney CO, White BF, Bruce BJ (1964) Acriflavine modification of nucleic acid formation, mutation induction and survival in ultraviolet light exposed bacteria. *Biochem Biophys Res Comm* 15(1):70–75
- Ankita T, Bipul CK, Sangita P, Raghwan K, Inderjeet K, Amit G, Asish KM, Suman KD (2020) Antibacterial action of acriflavine hydrochloride for eradication of the gastric pathogen helicobacter pylori. *FEMS Microbiol Lett* 367(21):1–14. <https://doi.org/10.1093/femsle/fnaa178> (PMID: 33118020)
- Valeria N, Agnieszka D, Kenji S, André M, Emilia B, Malgorzata B, Pawel B, Stefanie B, Mark B, Yuliya C, Anna C, Grzegorz D, Tony F, Michael H, Malwina J, Alex M, Katarzyna O, Magdalena P, Oliver P, Jan P, Ina R, Florian S, Artur S, Kristin G, Bjorn B, Michael S, Kamyar H, Grzegorz MP, Krzysztof P (2021) Acriflavine as betacoronavirus inhibitor. *BioRxiv Prepr*. <https://doi.org/10.1101/2021.03.20.436259>
- Nehme R, Hallal R, El Dor M, Kobeissy F, Gouilleux F, Mazurier F, Zibara K (2020) Repurposing of acriflavine to target chronic myeloid leukemia treatment. *Curr Med Chem* 27:1–15. <https://doi.org/10.2174/0929867327666200908114411>
- Saha RP, Sharma AR, Singh MK, Samanta S, Bhakta S, Mandal S, Bhattacharya M, Lee SS, Chakraborty C (2020) Repurposing drugs, ongoing vaccine, and new therapeutic development initiatives against COVID-19. *Front Pharmacol* 11:1258
- Shamsi A, Mohammad T, Anwar S, Amani S, Khan MS, Husain FM, Rehman MT, Islam A, Hassan MI (2021) Potential drug targets of SARS-CoV-2: from genomics to therapeutics. *Intl J Bio Macromol* 177:1–9
- Shin D, Mukherjee R, Grewe D, Bojkova D, Baek K, Bhattacharya A, Schulz L, Widera M, Mehdipour AR, Tascher G, Geurink PP, Wilhelm A, Gerbrand JVV, Ovaa H, Müller S, Knobloch K, Rajalingam K, Schulman BA, Cinatl J, Hummer G, Ciesek S, Dikic V (2020) Papain-like protease regulates SARS-CoV-2 viral spread and innate immunity. *Nature* 587:657–662
- Song S, Kwon OS, Chung YB (2005) Pharmacokinetics and metabolism of acriflavine in rats following intravenous or intramuscular administration of AG60, a mixture of acriflavine and guanosine, a potential antitumour agent. *Xenobiotica* 35:755–773
- Spiliopoulou N, Kokotos CG (2021) Photochemical metal-free aerobic oxidation of thiols to disulfides. *Green Chem* 23:546–551. <https://doi.org/10.1039/D0GC03818K>
- Choi YM, Xia WS, Park J, Lin MC (2000) Kinetics and mechanism for the reaction of phenyl radical with formaldehyde. *J Phys Chem A* 104:7030–7035
- Chakraborty M, Mandal PC, Mukhopadhyay S (2012) Mechanistic studies on the oxidation of thiols by a  $[Mn_4O_6]^{4+}$  core in aqueous acidic media. *Polyhedron* 45(1):213–220
- Chakraborty M, Mandal PC, Mukhopadhyay S (2013) Kinetic studies on oxidation of L-cysteine and 2-mercaptoethanol by a trinuclear Mn(IV) species in aqueous acidic media. *Inorg Chimica Acta* 398:77–82
- Sami P, Venkateshwari K, Mariselvi N, Sarathi A, Raja-sekaram K (2009) Studies on electron transfer reaction of heteropoly 11-tungstophosphophovanadate (V) by L-cysteine and thioglycolic acid in aqueous acid medium. *Trans Met Chem* 34:733–737
- Nowduri A, Adari KK, Gollapalli NR, Parvataneni V (2009) Kinetics and mechanism of oxidation of L-cysteine by hexacyanoferrate(III) in alkaline medium. *E-J Chem* 6(1):93–98
- Abdulsalam S, Idirs SO, Shallangwa GA, Onu AD (2020) Reaction of n, n<sup>1</sup>-phenylenebis(salicylideneiminato)cobalt(III) and L-cysteine in mixed aqueous medium: kinetics and mechanism. *Heliyon* 6:4. <https://doi.org/10.1016/j.heliyon.2020.e03850>
- Nkole IU, Osunkwo CR, Onu AD, Idris SO (2018) Kinetics and mechanism of the reduction of n-(2-hydroxyethyl)ethylenediamine triacetateiron(III) complex by thioglycol in bicarbonate buffer medium. *Intl J Adv Chem* 6(1):102–107. <https://doi.org/10.14419/ijac.v6i1.10902>
- Saha B, Hung M, Stanbury DM (2002) Reduction of octacyanomolybdate(V) by thioglycolic acid in aqueous media. *Inorg Chem* 41(21):5538–5543
- Santos MLd, Albin E, Corazza ML, Krieger N, Voll FAP (2021) Kinetics of enzymatic cetyl palmitate production by esterification with fermented solid of burkholderia contaminans in the presence of organic solvent. *Reac Kinet Mech Catal* 132:139–153. <https://doi.org/10.1007/s11144-020-01889-3>
- Sivasubramanian VK, Ganesan M, Rajagopal S, Ramaraj R (2002) Iron(III)-Salen complexes as enzyme models: mechanistic study of oxo(salen)iron complexes oxygenation of organic sulfides. *J Org Chem* 67:1506–1514

23. Onu AD, Iyun JF, Idris OS (2015) Kinetics and stoichiometry of the reduction of hydrogen peroxide by an aminocarboxylato-cobaltate(II) complex in aqueous medium. *Open J Inorg Chem* 5:75–82. <https://doi.org/10.4236/ojic.2005.54009>
24. Osunkwo CR, Nkole IU, Onu AD, Idris SO (2018) Electron transfer reaction of tris-(1,10-phenanthroline)cobalt(III) complex  $[\text{Co}(\text{phen})_3]^{3+}$  and thiosulphate ion ( $\text{S}_2\text{O}_3^{2-}$ ) in an aqueous acidic medium. *Intl J Adv Chem* 6(1):121–126. <https://doi.org/10.14419/ijac.v6i1.11326>
25. Nkole IU, Osunkwo CR (2019) Kinetic approach to the reduction of ethylenediaminetetraacetateferrate(III) complex by iodide ion in aqueous acidic medium. *Asian J Phys Chem Sci* 7(2):1–8
26. Idris SO, Tanimu A, Iyun JF, Mohammed Y (2015) Kinetics and mechanism of the reaction of malachite green and dithionite ion. *Intl Res J Pure Appl Chem* 5(2):177–184
27. Sun J, Stanbury DM (2002) Kinetics and mechanism of oxidation of thioglycolic acid by hexachloroiridate(IV). *J Chem Soc Dalton Trans* 5:785–791
28. Shanmugaprabha T, Selvakumar K, Rajasekaran K, Sami P (2016) A kinetic study of the oxidations of 2-mercaptoethanol and 2-mercaptoethylamine by heteropoly 11-tungsto-1-vanadophosphate in aqueous acidic medium. *Trans Met Chem* 41(1):77–85
29. Nkole IU, Abdulsalam S, Ibrahim I, Arthur DE (2021) Micellar effect on electron transfer reaction of 2-(hydroxyethyl)ethylenediaminetriacetatoiron(III) complex with thiocarbonate ion: kinetic model. *Chem Afr*. <https://doi.org/10.1007/s42250-021-00241-z>
30. Arthur DE, Nkole IU, Osunkwo CR (2020) Electron transfer reaction of tris(1,10-phenanthroline)cobalt(III) complex and iodide ion in an aqueous acidic medium. *Chem Afr* 4(1):63–69. <https://doi.org/10.1007/s42250-020-00201-z>
31. Ibrahim I, Idris SO, Abdulkadir I, Onu AD (2019) Kinetics and mechanism of the redox reaction of n, n'-phenylenebis-(salicylideneiminato)iron(III) with oxalic acid in mixed aqueous medium. *Trans Met Chem* 44(3):269–273